ADVANCED MATERIALS INTERFACES
Open Access
www.advmatinterfaces.de



# In Situ Infrared and UV–Vis Ellipsometries to Probe The Varnish Ageing and Swelling of G. Bellini *"Transfiguration"*

*Hélène Pasco, Arnaud Lesaine, Angela Cerasuolo, Cédric Boissière, Philippe Walter, Clément Sanchez, Laurence de Viguerie,* and Marco Faustini**

**Varnish layers are optical coatings that act as physico-chemical barrier between the historical paint layers and the environment. Understanding how varnish materials protect historical paintings over time and in the presence of humidity or organic vapors is of central importance for art preservation. However, probing the behavior of varnish after aging in real conditions remains a challenge. Here the question is addressed by "reshaping" the varnish material from the masterpiece of G. Bellini, the "*Transfiguration*", into an optical layer; coupling in situ Ultraviolet-Visible (UV–vis) and Infrared (IR) ellipsometries, the chemical state is correlated, optical properties and swelling of the varnish in presence of water and organic vapors. It shows that the varnish material aged since the 1950s still exhibits effective water repellence. The methodology may be applied to other relevant historical systems beyond paintings and may help in establishing more efficient preservation strategies for historical artworks.**

## 1. Introduction

Varnishes are optically transparent layers applied to the surface of a painting, to make it "bright, beautiful and completely lasting",[1] according to the monk Theophilus, already in the 12th century, describing their two main purposes.[2–6] First, varnishes modify the appearance of the painting by acting on the saturation of the colors and the gloss. Second, they are used to protect the surface and represent a physical barrier between the paint layers and the environment, preventing them from mechanical damage or UV-induced photochemical reactions. However, varnishes are considered "the most vulnerable parts of old master paintings"[5] and can be endangered by environmental effects (humidity, solvent action) or aging processes. Research aimed at preserving the protection afforded by varnish layers and the assessment of risks under storage conditions and during cleaning procedures is crucial to the field.[3] However, since the pioneering work of Stolow in 1954[7] and later of A. Phenix (in the 2000s)[8] many technical and theoretical drawbacks ("the fact that there is no (analytical) technique capable of measuring the action of solvents under realistic processing conditions", according to Baij et al.)[6] have prevented the community from making progress in understanding the action of solvents on oil paints and varnishes. Fife et al.[9] used NMR Mouse to probe the action of solvent cleaning directly on historical paintings, but with limited time and depth resolution, which prevents from in situ monitoring in thin layers. Then, some very recent works have emerged that highlight the high stakes and community interest in developing a reliable technique to ensure proper risk assessment focusing on paint layers[10] or varnishes:[11] Castel et al.[11] used neutron reflectometry, combined with AFM, to study the swelling of water and water+solvent in an ultra-thin layer of synthetic varnish. So far the aforementioned methods have been applied to modern varnishes used as model systems although they are not fully representative of the degraded varnish materials present on historical paintings.

As degraded varnishes exhibit altered optical properties that modify the visual appearance of the painting, they are often removed during restoration. The cleaning action, as the first step of a restoration, usually consists of the removal of surface dirt, commonly done with aqueous solutions, and if necessary, the removal of aged and discolored varnish by using organic solvents. This cleaning step is traditionally carried out using cottons, which are usually discarded after the operation but can be investigated further as they contain valuable information about the materials removed. Herein we present a methodology to gain additional

H. Pasco, A. Lesaine, P. Walter, L. de Viguerie
Laboratoire d'Archéologie Moléculaire et Structurale LAMS
Sorbonne Université
CNRS, 4 pl. Jussieu, Paris 75005, France
E-mail: laurence.de_viguerie@sorbonne-universite.fr
H. Pasco, A. Lesaine, C. Boissière, C. Sanchez, M. Faustini
Laboratoire Chimie de la Matière Condensée de Paris LCMCP
Sorbonne Université
CNRS, 4 pl. Jussieu, Paris 75005, France
E-mail: marco.faustini@sorbonne-universite.fr
A. Cerasuolo
Museo e Real Bosco di Capodimonte
Naples 80131, Italy
M. Faustini
Institut Universitaire de France (IUF)
Paris 75231, France

The ORCID identification number(s) for the author(s) of this article can be found under https://doi.org/10.1002/admi.202300563



**DOI: 10.1002/admi.202300563**

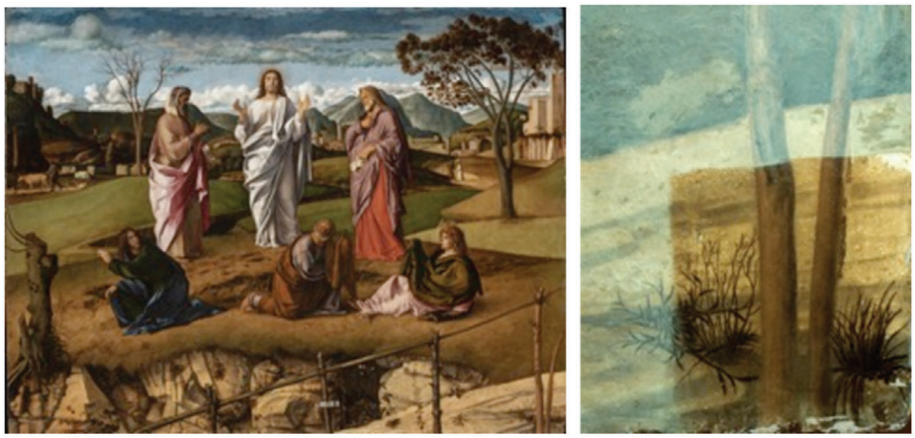

**Figure 1.** Giovanni Bellini, *Transfiguration* (Naples, Capodimonte museum), 1479. Photograph after restoration (left), and of a zone during restoration, involving varnish removal (right).

insight into varnish materials extracted from historical paintings, aged under real conditions, combining for the first time UV–vis and infrared environmental ellipsometry to monitor changes in their thickness, optical properties, and chemical composition. Latest developments have demonstrated the versatility of in situ ellipsometry (with controlled atmosphere) which makes it the appropriate tool here.[12] Far from the field of cultural heritage, several teams such as Papanu et al.[13] or Ogieglo et al.[14] have set up ellipsometric devices to study the swelling of thin polymer films. In addition, current advances in infrared ellipsometry[15] open up new possibilities to highlight chemical changes at play.

## 2. Results and Discussion

As a "proof of concept", we present the investigation of the varnish removed from the *Transfiguration*, masterpiece from Giovanni Bellini painted in 1478–1479 and exhibited in the Capodimonte museum (Naples, Italy), **Figure 1**a. Our strategy is illustrated in **Figure 2** and consists of several steps:

1) During restoration, the top historical varnish layer is removed manually with cottons (Figure 1b). In the present case, this varnish layer was applied during the previous restoration carried out in the 1950s; reports of the conservation department indicate the use of natural resins (mainly mastic and dammar) spirit varnishes (Figure S1, Supporting Information) typically composed of polymeric fraction and numerous triterpenoids.
2) The material composing the varnish is extracted from the cottons in a solution of $CH_2Cl_2/CH_3OH$; the solution is then dried and the material redispersed in turpentine.
3) An optical layer is fabricated by dip-coating deposition on a Silicon wafer.

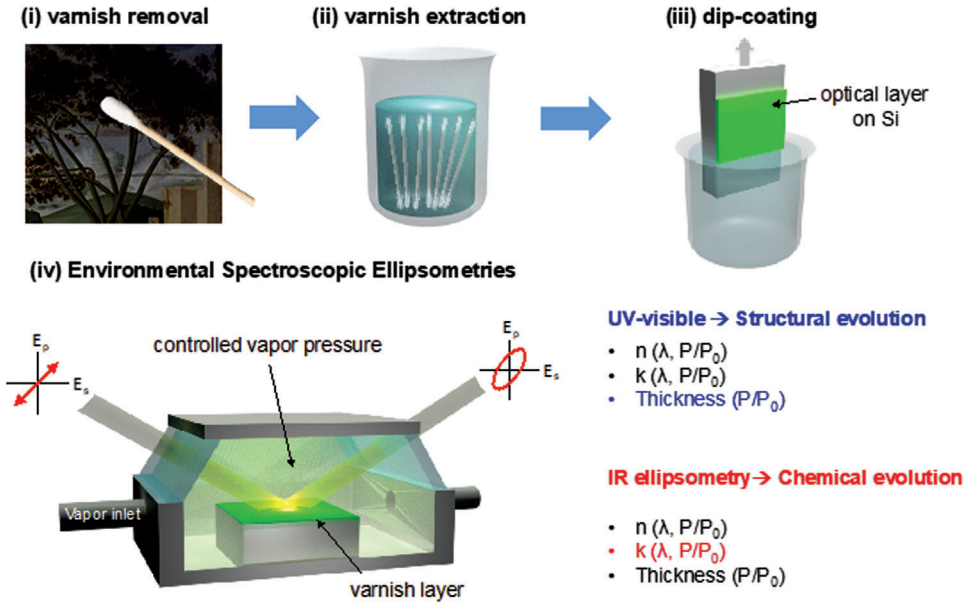


**Figure 2.** An analytical approach based on UV–vis and IR environmental spectroscopic ellipsometries applied on "reshaped" historical varnish material.

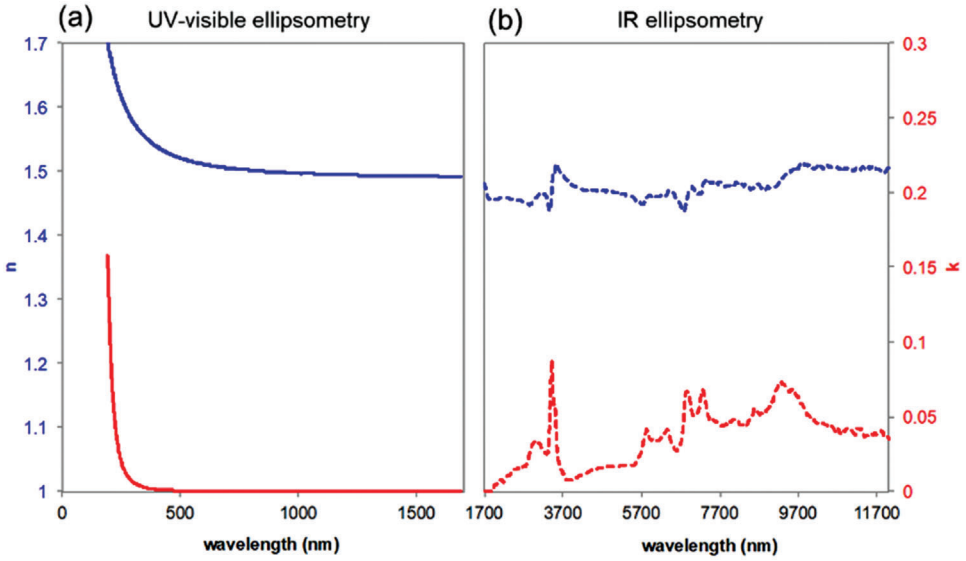


**Figure 3.** Optical properties of the "historical varnish" material. Evolution of the refractive index (n, blue plot) and extinction coefficient (k, red plot) determined by a) UV–vis and b) IR ellipsometries.

4) The optical films obtained by dip-coating, composed of the varnish material recovered from the *Transfiguration*, are then studied by in situ environmental UV–vis–NIR (300–1700 nm) and IR ellipsometries (1700–12500 and 5882-800 $cm^{-1}$ in this study).

The basic principle of spectroscopic ellipsometry is the same in the two cases: during an ellipsometric experiment, polarized light beam interacts with the film. This interaction changes the state of polarization of the reflected light. Measurements of the initial and final states of polarization are parametrized by the interference amplitude component Ψ and the phase difference Δ. The Ψ and Δ curves are then fitted by using optical models to determine the refractive index (n) and the extinction coefficient (*k*) as function of the wavelength and thickness. While both UltraViolet-Visible-NearInfraRed (UV–vis–NIR) and IR ellipsometries provide evolution of n, k, and thickness as function of the wavelength and vapor pressure ($P/P_0$); they provide complementary insights. UV–vis ellipsometry is more accurate for determining the thickness for films of ≈300 nm. In the IR ellipsometry, Ψ and Δ curves values are very sensitive to photons absorptions due to vibrational modes at IR wavelengths allowing to monitor precise evolution of the chemical composition into the film.

Ellipsometric measurement is not destructive and is ideally suited for environmental analysis. As illustrated in the Figure 2iv, in the present study, the ellipsometric study was performed in an environmental chamber that enables controlling the partial vapor pressure in the atmosphere around the varnish film.[16] While UV–vis–NIR environmental ellipsometry was previously used to monitor structural change in thin films (swelling, porosimetry, etc),[17] we introduce for the first time environmental IR ellipsometry to follow the chemical evolution of films. Since IR ellipsometry is based on polarization differences, we can probe exclusively the evolution of the vibrational modes in the films avoiding the possible contribution of the surrounding atmosphere. In the following, we refer to the material reworked from the historical painting the *Transfiguration* as "historical varnish", although being transformed in the process of extraction, as opposed to the model varnishes prepared from a commercial mastic resin.

### 2.1. Optical Constant of the "Historical Varnish"

We first probed the optical constants of the "historical varnish" from the UV to the IR ranges (300–11700 nm) by measuring at three different angles 60°, 65°, and 70°. In general, except in the UV, the *n* value is closed to 1.5 (in agreement with values reported for mastic and dammar resins).[18,19]

**Figure** 3a shows that the film is strongly absorbing in the UV range (k >0) and optically transparent in the visible range (k = 0). In the transparent part (400–1000 nm), the curves were fitted by Cauchy-Urbach tail dispersion relation for the refractive index to obtain an accurate value of thickness (Figure S2, Supporting Information). This is crucial to extract the value of n and k in the IR range where many absorption peaks are present. After determining the thickness from the transparent part of the data, the optical constants for the entire spectrum, including the multiple absorbing peak in the IR, can be found by B-spline parametrization (Figure S3, Supporting Information), a convenient mathematical description of the dielectric function.[20,21] In the IR, the k curves as function of the wavelength shown in Figure 3b present several peaks that are associated to vibrational peaks. To confirm the accurateness of the IR ellipsometric measurement, the k value obtained by IR ellipsometry, (**Figure** 4b), was compared with the IR absorbance spectrum, determined by conventional ATR-FTIR spectroscopy (Figure 4a). Before discussing the results, two important aspects need to be specified. First, while the *k* curves in Figures 3b and 4b appear different, they represent the same experimental data plotted as function of the wavelength (red curve in Figure 3b) or of the wavenumber (Figure 4b). Second, it is important to remind that n and k

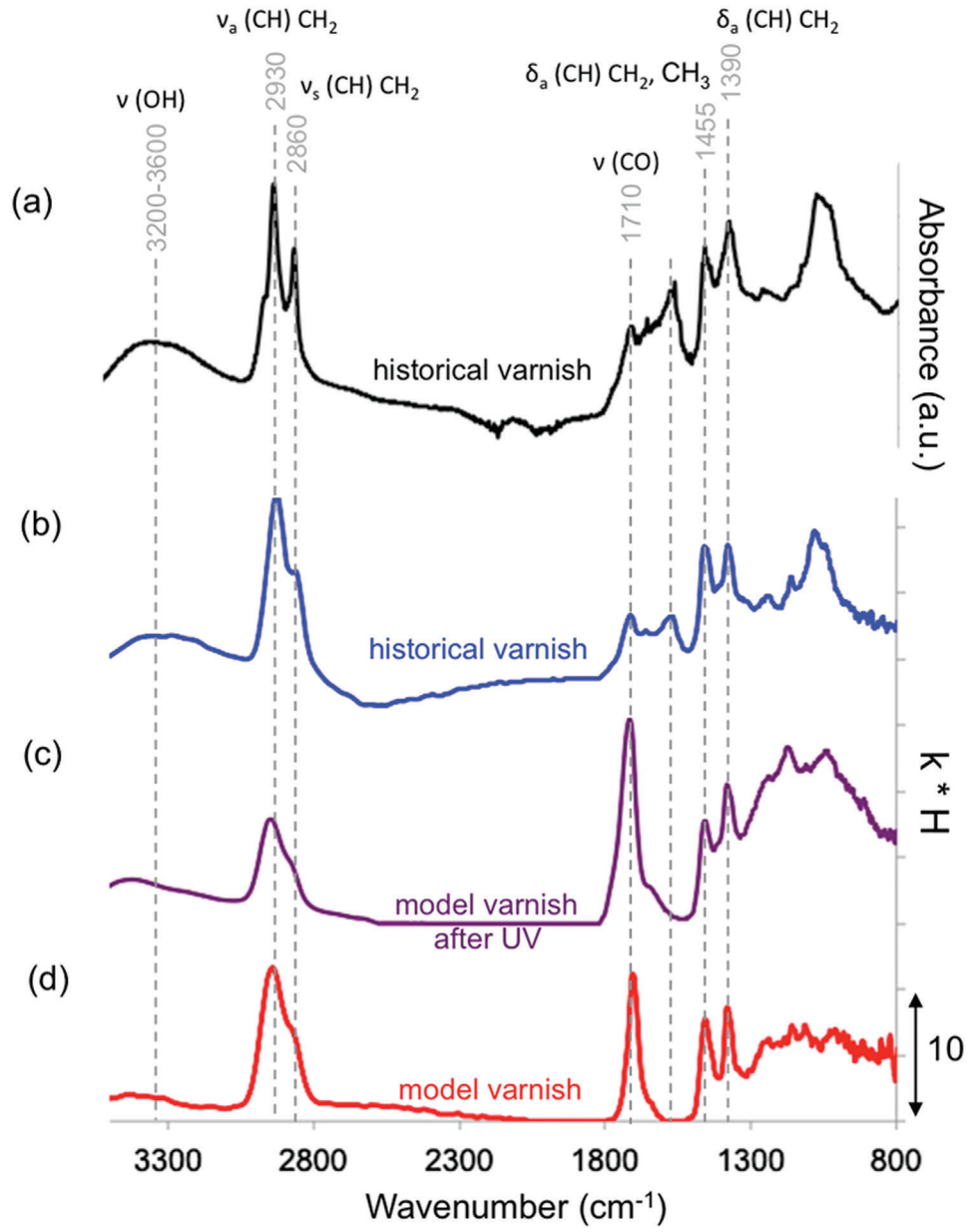


**Figure 4.** IR spectrum of: a) "historical varnish" material determined by conventional ATR-FTIR spectroscopy, b) c) and d) varnish material determined by IR ellipsometry: b) "historical varnish", c) model varnish after UV, and d) model varnish. It is important to note that, the scalebar value of 10 is added as a reference to compare the intensity of the k*H values of curves b, c, d.

are dimensionless numbers characterizing the propagation of electromagnetic waves in a given unit of volume. In order to compare the optical properties of films having different thicknesses (and thus volumes), the *k* values must be multiplied by the thickness (H). In Figure 4, and in the following analyses, the k value obtained by ellipsometry is thus multiplied by H. Oppositely, the absorption spectrum obtained by conventional Attenauted Total Reflectance Fourier Transform InfraRed (ATR-FTIR) spectroscopy in Figure 4a is simply plotted as arbitrary units and presents narrower peaks and a generally higher spectral resolution. Nevertheless, the two curves obtained by ATR-FTIR Figure 4a and IR ellipsometry Figure 4b are impressively similar considering that the two spectra have been obtained from the same material but with two different techniques and different samples (bulk versus film).

### 2.2. Infrared Ellipsometry of Modern and "Historical" Varnishes

A modern mastic varnish (prepared by dissolution of mastic resin (10 wt.%) in turpentine) was also prepared and a 250 nm–thick film was studied by IR ellipsometry. The k curve of this model varnish is presented in Figure 4d. The k values were multiplied by

the thickness (H) in order to compare the contribution of the two films, providing a better understanding of the observed vibration bands in the "historical varnish". Similar peaks can be observed assigned to terpenic resins (($\nu$CO) at *ca.* 1710 $cm^{-1}$, ($\nu$(CH) $CH_2$) at *ca.* 2860 and 2930 $cm^{-1}$ (respectively anti-symmetric and symmetric ones), as well as ($\delta$(CH) $CH_3/CH_2$) at 1455 and ($\delta$(CH) $CH_3$) at 1390 $cm^{-1}$ (both anti-symmetric)).[22] The possible presence of oil cannot be ruled out as the CO band is very broad with a shoulder at 1740 $cm^{-1}$; it is difficult to conclude as the triglycerides characteristic peaks in 1000–1200 $cm^{-1}$ range may be overlapping oxidation features from the resin compounds. Differences between the IR spectra of the "historical varnish" and the one of the model varnish can be explained by oxidation processes during the ageing of the varnish. To probe and confirm the effect of oxidative ageing, the model varnish system was artificially aged by exposure to UV (280–315 nm) for 10 min (225 $mW.cm^{-2}$), and the resulting infrared spectrum is indicated in Figure 4c. UV exposure is known to promote oxidation processes and can help to predict the evolution of chemical, optical, and mechanical properties of systems highly sensitive to oxidation such as varnishes.[24,25] As described in the literature,[22–29] the absorbance between 3200 and 3600 $cm^{-1}$, assigned to OH bonds, increases due to oxidation reactions. Furthermore, the absorbance of the fingerprint zone increases between 1330 and 800 $cm^{-1}$ due to C—O stretching absorption. Moreover, the artificial aging of triterpenic varnishes and resins leads to the broadening of the carbonyl band.[22,28] In parallel, a decrease of the CH characteristic bands has been reported by different authors[22–29] very visible in the spectrum of the aged model varnish. Also commented in the literature, the bands at ca. 1455 $cm^{-1}$ ($\delta_a$(CH) $CH_3/CH_2$) undergo to a slight decrease in comparison to the one at 1385–1380 $cm^{-1}$ ($\delta_a$(CH) $CH_2$), "evolution linked with ring-opening reactions, fragmentation and condensation of the original triterpenoid compounds".

Additional bands are also visible in the spectrum of the "historical varnish" compared to the model varnish. First of all, a broad band at ca. 1580 $cm^{-1}$ is present which can be hardly explained by any organic component of varnish. As it lies in the characteristic range of Cu carboxylates ($\nu$(CO)), additional XRF measurements were carried out on the film and on the de-varnishing cottons which confirmed the presence of Cu (Figure S4, Supporting Information). This is not surprising considering that Cu-based pigments were widely used by G. Bellini in his works.[23] The presence of Cu-carboxylated species in the varnish layer may be due to the migration of Cu-carboxylate from the paint layers or to the reaction between the resin/varnish and the Cu-based pigments.[24–26] Moreover, if the global intensity of the 1330–800 $cm^{-1}$ zone increases with oxidation, a band at ca. 1085 $cm^{-1}$ seem also present, which can be linked to an additional compound, such as cellulose remaining from the cottons.[30]

### 2.3. Swelling Properties

The "historical varnish" film was then investigated by in situ ellipsometry in the presence of vapors of isopropyl alcohol (IPA), commonly used in restoration protocols and chosen because, with respect to other relevant solvents, it presents a characteristic IR signature not overlapping with those of the varnish material

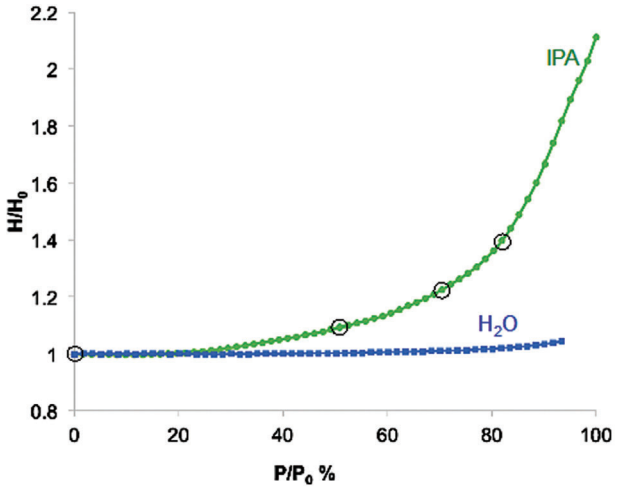


**Figure 5.** Vapor-induced swelling (water versus IPA) of the "historical varnish".

(≈950 $cm^{-1}$). Water vapor was also used to probe the water repellence of the "historical varnish". **Figure 5** shows the evolution of the relative thickness $H/H_0$ as a function of vapor pressure P/P0 for the two solvents obtained by UV–vis ellipsometry. In presence of saturated IPA, the film exhibits swelling curve that is typical of polymer materials. The thickness increases drastically starting from 30 % IPA by doubling the thickness in saturated conditions. This is not surprising considering that such solvent is used to dissolve varnish layers. Decreasing the $\%P/P_0$, the process is generally reversible as shown in in Figure S5 (Supporting Information). The plot displays the evolution of Δ curves at 0% IPA and 100% IPA for the adsorption and desorption experiments; the initial and final curves are indeed very similar confirming that the film comes back to its initial state after swelling/deswelling. In comparison, at first sight, the "historical varnish" layer does not swell much in the presence of water vapor (Figure 5).

To gain better insights and prove the full potential of the methodology, the same experiment was performed by environmental IR ellipsometry with IPA vapors (Figure S6, Supporting Information). **Figure 6a** shows the Ψ and Δ curves of the film at four representative P/P0% (0%, 50%, 70%, and 80 %). The curves present an oscillation due to constructive interferences generated at the substrate-film-air interfaces. In addition, typical signatures of vibrational absorption are visible. In particular, we have analyzed in detail two spectral ranges characteristic of IPA molecules adsorbed into the films: the C—H stretching of the aliphatic chain at 2930 ($\nu_a$ (CH) $CH_2$) and the C—O stretching at ≈950 $cm^{-1}$. In this case, the Ψ and Δ curves were fitted with optical models based on Lorentz oscillators that enable evaluating the contributions of the (overlapping) vibrational modes. For instance, Figure 6b shows the k peaks convolution in the region 3500-2800 $cm^{-1}$ in which several contributions can be accounted. Among the different vibrational modes that can be found in that region, we selected the $\nu_s$ (CH) $CH_2$, $\nu_a$ (CH) $CH_2$, and the $\nu$(OH), the main contributions that have been identified in Figure 4. The experimental and fitted Ψ and Δ curves in the 3500–2800 $cm^{-1}$ region corresponding to Figure 6b are reported in Figure S7 (Supporting Information).

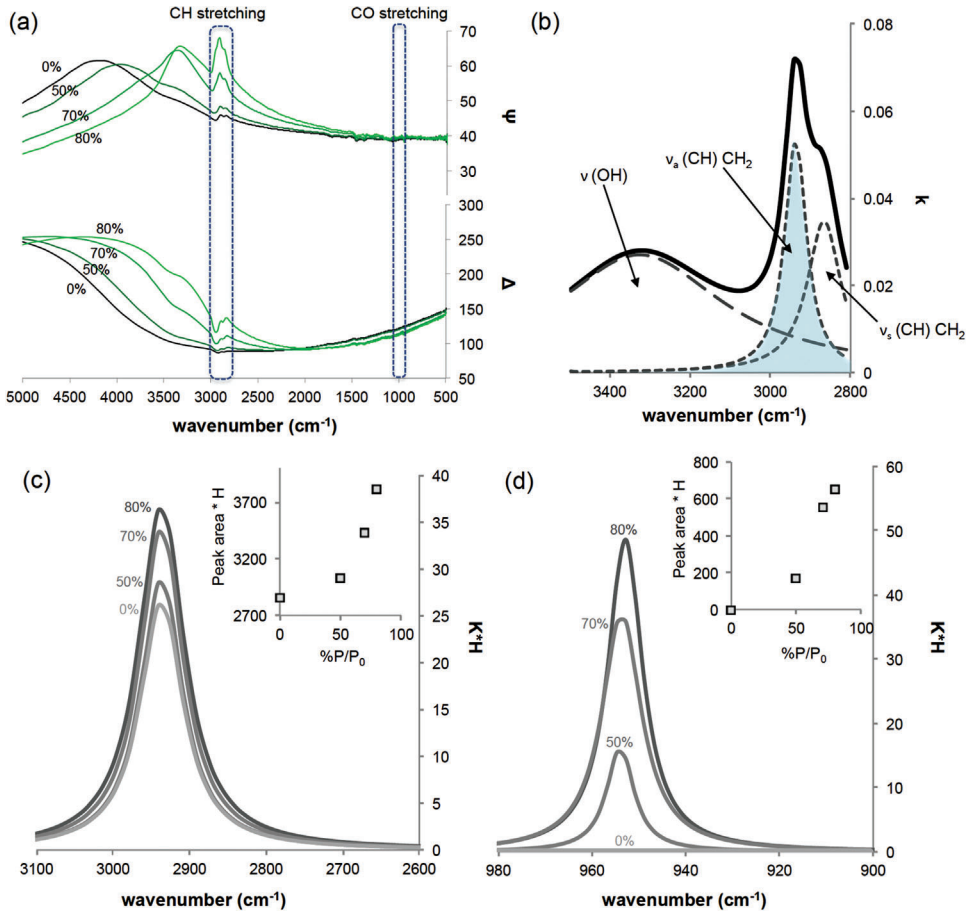


**Figure 6.** In situ IR ellipsometry during IPA exposure. a) Ψ and Δ curves, b) convolution of peaks at 50 % IPA, c) fitted ($\nu_a$(CH) $CH_2$) stretching peak, d) fitted CO stretching peak.

The present technique enables monitoring the evolution of k versus $P/P_0$ for specific vibrations of the $\nu_a$(CH) $CH_2$ peak contribution (highlighted in blue in Figure 6b) and the C—O stretching as shown in Figure 6c,d respectively. While C—H signal at 2930 $cm^{-1}$ was already present in the varnish at 0% IPA, the signal of C—O stretching ≈950 $cm^{-1}$ (Figure 6d) is exclusively due to IPA absorption (as indicated above, the $\nu$(C—O) broadband in the "historical varnish" is centered ≈1085 $cm^{-1}$). In both cases, the intensity of k peak increases due to IPA uptaken into the film. In order to compare these values, it is important to remind that n and k are dimensionless numbers characteristic of a given unit of volume.

Since the volume of the films increases during the experiment, the k peak area must be multiplied for the thickness for each $P/P_0$. As shown in the insets in Figure 6c,d the amount of IPA in the film increases similarly. After IPA desorption in dry air, the films come back reversibly to its initial state suggesting that no residual solvent remains physisorbed in the varnish layer after this experiment, and that no irreversible chemical reaction occurred during the swelling. Coming back to Figure 5, the "historical varnish" material swells only slightly in presence of water as compared to organic solvent. However, water repellency of the varnish layer has evolved over time. To proof that, we compare the humidity-driven swelling of the modern mastic varnish (not aged) and the "historical varnish" whose resin has aged since the 1950s. Looking at swelling curves ($H/H_0$) in presence of humidity (**Figure 7**), the two films exhibit different behaviors: the model

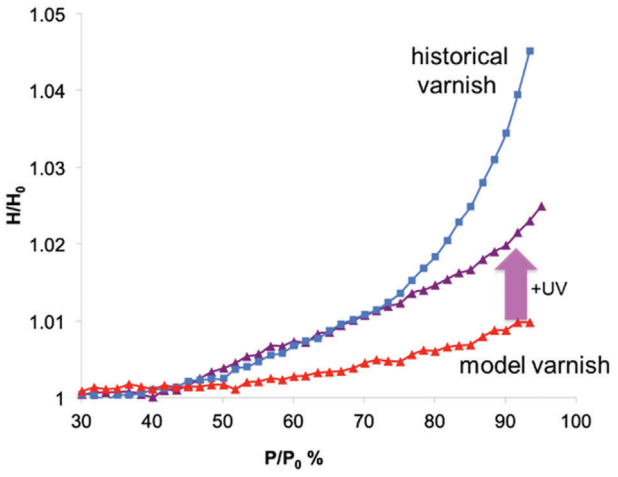


**Figure 7.** Water vapor swelling behavior of the "historical varnish" material compared with the model and UV-aged varnishes.

mastic varnish layer swells less than 1% at high relative humidity ($P/P_0$ above 0.9) while the swelling of the "historical varnish" is more than four times higher. After artificial aging under UV, the swelling of the mastic varnish layer is twice higher and the swelling curve under 75% is similar as the one of the varnish coming from Bellini's artwork, confirming the effect of oxidation on the swelling properties.

## 3. Conclusion

In summary, we present here a new methodology to study the optical, chemical, and sorption behavior of aged resins extracted from historical paintings. In the case of G. Bellini's *Transfiguration*, we show that the varnish materials aged since the 1950s still exhibit effective water repellance. Transforming the material into an optical coating makes it possible to combine UV and IR ellipsometry and monitor the impact of changing environmental conditions, which is a current challenge for the community, as evidenced by very recent developments in the field.[10,11] This approach represents a further progress towards a more realistic understanding of the effect of environmental conditions on varnishes. It is also an important step towards the study of varnish layers directly on historical works, an exciting line of future research.

## 4. Experimental Section

*Ellipsometry Instruments*: The UV–vis analyses were carried out on a Variable Angle Spectroscopic Ellipsometer (VASE from J.A. Wollam Co., Inc.) in the UV–vis–NIR range 300–1700 nm at three incident angles (60°, 65°, and 70°). The IR measurements were performed with a Mark II ellipsometer (J.A. Wollam Co., Inc.) in the range 1700–12500 nm. The acquisitions were performed using the VASE software. A typical IR ellipsometric measurement requires acquisition times of the order of tens of minutes depending on the amount of matter present on the films and on the targeted spectral resolution. Typically, the in situ experiments were made with an acquisition time of 28 min. In this configuration, the IR ellipsometric measurement generally presents a lower spectral resolution as compared to ATR. The spectral resolution of the IR ellipsometric measurement could be improved by increasing the acquisition time up to some hours. Since, n and k were dimensionless numbers, in order to compare the optical properties of films having different thicknesses, the n and *k* values were multiplied by the thickness (H).

*In Situ Ellipsometry Set-Up*: To perform the in situ measurements (controlled atmosphere), the samples were place in an environmental chamber (equipped with two pinholes to allow the passage of light) installed on the stage of the ellipsometer. The chamber was linked to dry air ($N_2$, flow 5 L $min^{-1}$) and to two wash bottles connected in series containing the appropriate solvent, one at 50°C and the other at room temperature. These saturated vapors were then mixed with dried $N_2$ in a certain ratio that was determined by the mass flow controller (Solgelway) interfaced with a software Regul'Hum. The mixing ratio determines the $P/P_0$ in the chamber that was calibrated through a humidity sensor (in the case of $H_2O$) or by using reference samples (in the case of IPA).[31]

For water adsorption experiments, the ramp was 0% Relative Humidity (RH) (1 min), 100% RH in 20 min (1 min), 0% RH. For isopropyl alcohol exposure, the ramp for vapor pressure was $P = 0$ (1 min), $P = 0.95$ in 20 min (1 min), $P = 0$. Prolonged exposure at high $P/P_0$ (more than 30 min) should be avoided because it causes loss in film reflectivity attributed to the dewetting of the film.

*Film Preparation*: The "modern varnish" was prepared by mixing 10 wt% of commercial mastic resin (Kremer) in turpentine (Sennelier), a natural terpenic solvent. The "historical varnish" (dated from the 1950s) was removed from Bellini's painting with cottons by art restorers. Then, the cottons were soaked in a solution of $CH_2Cl_2/CH_3OH$ to extract the varnish. The solution obtained was finally dried and the residue was dissolved in turpentine.

The films were dip-coated with the varnishes on Silicon wafer previously activated by a plasma treatment. The deposition conditions have been optimized to fabricate films having thickness of ≈300 nm, stable in air even after several weeks (Figure S9, Supporting Information): low Relative Humidity (<10% RH using $N_2$ as dry air, T = 18–23 °C) and at a withdrawal speed of 5 mm·$s^{-1}$ to allow well-controlled thickness (about 300 nm).[32–34]

*ATR-FTIR Measurements*: The data have been collected with a Cary 630 spectrometer equipped with a 5-bounce ZnSe accessory. The spectra were acquired in the range 650–4000 $cm^{-1}$ with 32 scans and a spectral resolution of 4 $cm^{-1}$.

*X-Ray Fluorescence (XRF) Measurements*: In-house-built XRF instrument was used, featuring a Pd anode end window X-ray tube (Moxtek MAGNUM, Orem, UT) operated at 30 kV and 50 µA and a silicon drift detector (X-123FAST SDD, Amptek, Bedford, MA) with an active area of 25 $mm^2$ collimated to 17 $mm^2$ and a nominal thickness of 500 µm. The X-ray tube was connected to the detector via a holder produced by 3D printing. As a collimator primary optic, a Pd tube of 800 µm inner diameter was used, yielding a beam size of approximately 1.2 mm. The typical working distance was 1 cm. A digital microscope (Dino-lite, AnMo Electronics Corporation, New Taipei City, Taiwan) and a laser distance measurement device (OADM20, Baumer, Frauenfeld, Switzerland) allow for measuring the position of the primary beam on the surface of the object.

## Supporting Information

Supporting Information is available from the Wiley Online Library or from the author.

## Acknowledgements

The Ph.D. of H. P. was founded by the ED397 and the LabEx MiChem, part of the French state funds managed by the ANR within the investissements d'avenir program under reference ANR-11-10EX-0004-02. A.L. acknowledges funding from the Paris Ile-de-France Region–DIM Respore and DIM "Matériaux anciens et patrimoniaux". The infrared ellipsometry was funded by the Région Ile-de-France in the framework of DIM Respore and by the French state within the Investissements d'Avenir programme under reference ANR-11-IDEX-0004-02, within the framework of the Cluster of Excellence MATISSE.

## Conflict of Interest

The authors declare no conflict of interest.

## Data Availability Statement

The Data that support the findings of this study are available from the corresponding author upon reasonable request.

## Keywords

environmental ellipsometry, solvent, swelling, varnish

Received: June 29, 2023
Revised: October 16, 2023
Published online: December 19, 2023

[1] Theophilus, *On divers Arts* (Eds: J.G. Hawthorneand, C.S. Smith), *2*, Dover Publications, New York, USA **1963**.
[2] P. Walter, L. De Viguerie, *Nat. Mater.* **2018**, *17*, 106.
[3] J.-P. Echard, L. Bertrand, A. Von Bohlen, A.-S. Le Hô, C. Paris, L. Bellot-Gurlet, B. Soulier, A. Lattuati-Derieux, S. Thao, L. Robinet, B. Lavédrine, S. Vaiedelich, *Angew. Chem., Int. Ed.* **2010**, *49*, 197.
[4] J. Imbrogno, A. Nayak, G. Belfort, *Angew. Chem.* **2014**, *126*, 7134.
[5] E. R. De La Rie, *Anal. Chem.* **1989**, *61*, 1228A.
[6] L. Baij, J. Hermans, B. Ormsby, P. Noble, P. Iedema, K. Keune, *Herit. Sci.* **2020**, *8*, 43.
[7] N. Stolow, *J. Sci. Instrum.* **1954**, *31*, 416.
[8] A. Phenix, *J. Am. Inst. Conserv.* **2002**, *41*, 43.
[9] G. R. Fife, B. Stabik, A. E. Kelley, J. N. King, B. Blümich, R. Hoppenbrouwers, T. Meldrum, *Mag. Reson. Chem.* **2015**, *53*, 58.
[10] L. Baij, J. Buijs, J. J. Hermans, L. Raven, P. D. Iedema, K. Keune, J. Sprakel, *Sci. Rep.* **2020**, *10*, 10574.
[11] A. Castel, P. Gutfreund, B. Cabane, Y. Rharbi, *Soft Matter* **2020**, *16*, 1485.
[12] Z. Chehadi, C. Boissière, C. Chanéac, M. Faustini, *Nanoscale* **2020**, *12*, 13368.
[13] J. S. Papanu, D. W. Hess, A. T. Bell, D. S. Soane, *J. Electrochem. Soc.* **1989**, *136*, 1195.
[14] W. Ogieglo, H. Wormeester, M. Wessling, N. E. Benes, *Polymer* **2013**, *54*, 341.
[15] S. Dasgupta, S. Biswas, K. Dedecker, E. Dumas, N. Menguy, B. Berini, B. Lavedrine, C. Serre, C. Boissière, N. Steunou, *ACS Appl. Mater. Interfaces* **2023**, *15*, 60.
[16] M. R. Baklanov, K. P. Mogilnikov, V. G. Polovinkin, F. N. Dultsev, *J. Vac. Sci. Technol. B.* **2000**, *18*, 1385.
[17] C. Boissière, D. Grosso, S. Lepoutre, L. Nicole, A. Brunet Bruneau, C. Sanchez, *Langmuir* **2005**, *21*, 12362.
[18] E. R. de la Rie, *Stud. Conserv.* **1987**, *32*, 1.
[19] K. Polikreti, C. Christofides, *J. Cult. Herit.* **2006**, *7*, 30.
[20] J. W. Weber, T. A. R. Hansen, M. C. M. Van De Sanden, R. Engeln, *J. Appl. Phys.* **2009**, *106*, 123503.
[21] J. Mohrmann, T. E. Tiwald, J. S. Hale, J. N. Hilfiker, A. C. Martin, *J. Vac. Sci. Technol. B.* **2020**, *38*, 014001.
[22] C. Azémard, C. Vieillescazes, M. Ménager, *Microchem. J.* **2014**, *112*, 137.
[23] J. B. Dunkerton, National Gallery Technical Bulletin, Vol. *39*, *Giovanni Bellini's Painting Technique*, National Gallery Company, London, UK, **2018**.
[24] J. J. Boon, F. Hoogland, K. Keune, H. M. Parkin, AIC Paintings Specialty Group Postprints, American Institute for Conservation of Historic & Artistic Works, Washington, DC **2006**.
[25] T. Poli, O. Chiantore, E. Diana, A. Piccirillo, *Coatings* **2021**, *11*, 171.
[26] T. Poli, A. Piccirillo, M. Nervo, O. Chiantore, *J. Colloid Interf. Sci.* **2017**, *503*, 1.
[27] E. R. de la Rie, *Stud. Conserv.* **1988**, *33*, 53.
[28] P. Dietemann, M. Kälin, S. Zumbühl, R. Knochenmuss, S. Wülfert, R. Zenobi, *Anal. Chem.* **2001**, *73*, 2087.
[29] A. Nevin, D. Comelli, I. Osticioli, L. Toniolo, G. Valentini, R. Cubeddu, *Anal. Bioanal. Chem.* **2009**, *395*, 2139.
[30] D. Ciofini, PhD Thesis, Universita degli studi Firenze, Italy, **2015**.
[31] M. R. Derrick, D. Stulik, J. M. Landry, *Infrared Spectroscopy in Conservation Science*, Getty Publications, Los Angeles, USA **2000**.
[32] O. Dalstein, D. R. Ceratti, C. Boissière, D. Grosso, A. Cattoni, M. Faustini, *Adv. Funct. Mater.* **2016**, *26*, 81.
[33] E. Bindini, G. Naudin, M. Faustini, D. Grosso, C. Boissière, *J. Phys. Chem. C* **2017**, *121*, 14572.
[34] D. R. Ceratti, B. Louis, X. Paquez, M. Faustini, D. Grosso, *Adv. Mate.* **2015**, *27*, 4958.